

Increasing robustness of bipolar pulse coding in Brillouin distributed fiber sensors

Zhisheng Yang,^{1,2,*} Marcelo A. Soto,¹ and Luc Thévenaz¹

¹EPFL, Swiss Federal Institute of Technology, Institute of Electrical Engineering, SCI-STI-LT Station 11, CH-1015 Lausanne, Switzerland

²Permanent address: State Key Laboratory of Information Photonics & Optical Communications, Beijing University of Posts and Telecommunications, Beijing 100876, China

*zhisheng.yang@epfl.ch

Abstract: The robustness of bipolar pulse coding against pump depletion issues in Brillouin distributed fiber sensors is theoretically and experimentally investigated. The presented analysis points out that the effectiveness of bipolar coding in Brillouin sensing can be highly affected by the power unbalance between -1 's and $+1$'s elements resulting from depletion and amplification of coded pump pulses. In order to increase robustness against those detrimental effects and to alleviate the probe power limitation imposed by pump depletion, a technique using a three-tone probe is proposed. Experimental results demonstrate that this method allows increasing the probe power by more than 12.5 dB when compared to the existing single-probe tone implementation. This huge power increment, together with the 13.5 dB signal-to-noise enhancement provided by 512-bit bipolar Golay codes, has led to low-uncertainty measurements (< 0.9 MHz) of the local Brillouin peak gain frequency over a real remoteness of 100 km, using a 200 km-long fiber-loop and 2 m spatial resolution. The method is evaluated with a record figure-of-merit of 380'000.

©2016 Optical Society of America

OCIS codes: (060.2310) Fiber optics; (060.2370) Fiber optics sensors; (290.5900) Scattering, stimulated Brillouin; (060.4370) Nonlinear optics, fibers.

References and links

1. T. Horiguchi, K. Shimizu, T. Kurashima, M. Takeda, and Y. Koyamada, "Development of a distributed sensing technique using Brillouin scattering," *J. Lightwave Technol.* **13**(7), 1296–1302 (1995).
2. M. A. Soto and L. Thévenaz, "Modeling and evaluating the performance of Brillouin distributed optical fiber sensors," *Opt. Express* **21**(25), 31347–31366 (2013).
3. M. Alem, M. A. Soto, and L. Thévenaz, "Analytical model and experimental verification of the critical power for modulation instability in optical fibers," *Opt. Express* **23**(23), 29514–29532 (2015).
4. S. M. Foaeng and L. Thévenaz, "Impact of Raman scattering and modulation instability on the performances of Brillouin sensors," *Proc. SPIE* **7753**, 77539V (2011).
5. L. Thévenaz, S. F. Mafang, and J. Lin, "Effect of pulse depletion in a Brillouin optical time-domain analysis system," *Opt. Express* **21**(12), 14017–14035 (2013).
6. F. Rodriguez-Barrios, S. Martin-Lopez, A. Carrasco-Sanz, P. Corredra, J. D. Ania-Castanón, L. Thévenaz, and M. Gonzalez-Herraez, "Distributed Brillouin fiber sensor assisted by first-order Raman amplification," *J. Lightwave Technol.* **28**(15), 2162–2172 (2010).
7. S. Martin-Lopez, M. Alcon-Camas, F. Rodriguez, P. Corredra, J. D. Ania-Castañón, L. Thévenaz, and M. Gonzalez-Herraez, "Brillouin optical time-domain analysis assisted by second-order Raman amplification," *Opt. Express* **18**(18), 18769–18778 (2010).
8. M. A. Soto, G. Bolognini, and F. Di Pasquale, "Optimization of long-range BOTDA sensors with high resolution using first-order bi-directional Raman amplification," *Opt. Express* **19**(5), 4444–4457 (2011).
9. M. A. Soto, G. Bolognini, F. Di Pasquale, and L. Thévenaz, "Simplex-coded BOTDA fiber sensor with 1 m spatial resolution over a 50 km range," *Opt. Lett.* **35**(2), 259–261 (2010).
10. M. A. Soto, G. Bolognini, and F. Di Pasquale, "Analysis of pulse modulation format in coded BOTDA sensors," *Opt. Express* **18**(14), 14878–14892 (2010).
11. H. Liang, W. Li, N. Linze, L. Chen, and X. Bao, "High-resolution DPP-BOTDA over 50 km LEAF using return-to-zero coded pulses," *Opt. Lett.* **35**(10), 1503–1505 (2010).
12. M. A. Soto, S. Le Floch, and L. Thévenaz, "Bipolar optical pulse coding for performance enhancement in BOTDA sensors," *Opt. Express* **21**(14), 16390–16397 (2013).

13. S. Le Floch, F. Sauser, M. A. Soto, and L. Thévenaz, "Time/frequency coding for Brillouin distributed sensors," *Proc. SPIE* **8421**, OFS-2012, 84211J (2012).
14. S. Le Floch, F. Sauser, M. Llera, and E. Rochat, "Novel Brillouin optical time-domain analyzer for extreme sensing range using high power flat frequency coded pump pulses," *J. Lightwave Technol.* **33**(12), 2623–2627 (2015).
15. S. Le Floch, F. Sauser, M. Llera, M. A. Soto, and L. Thévenaz, "Colour simplex coding for Brillouin distributed sensors," *Proc. SPIE* **8794**, *Fifth European Workshop on Optical Fibre Sensors (EWOFS)*, 879437 (May 20, 2013).
16. M. A. Soto, G. Bolognini, and F. Di Pasquale, "Simplex-coded BOTDA sensor over 120 km SMF with 1 m spatial resolution assisted by optimized bidirectional Raman amplification," *IEEE Photonics Technol. Lett.* **24**(20), 1823–1826 (2012).
17. M. A. Soto, X. Angulo-Vinuesa, S. Martin-Lopez, S.-H. Chin, J. D. Ania-Castanon, P. Corredera, E. Rochat, M. Gonzalez-Herraez, and L. Thévenaz, "Extending the real remoteness of long-range Brillouin optical time-domain fiber analyzers," *J. Lightwave Technol.* **32**(1), 152–162 (2014).
18. Y. Dong, L. Chen, and X. Bao, "Extending the sensing range of Brillouin optical time-domain analysis combining frequency-division multiplexing and in-line EDFAs," *J. Lightwave Technol.* **30**(8), 1161–1167 (2012).
19. Y. London, Y. Antman, R. Cohen, N. Kimelfeld, N. Levanon, and A. Zadok, "High-resolution long-range distributed Brillouin analysis using dual-layer phase and amplitude coding," *Opt. Express* **22**(22), 27144–27158 (2014).
20. N. Levanon, "Noncoherent pulse compression," *IEEE Trans. Aerosp. Electron. Syst.* **42**(2), 756–765 (2006).
21. M. D. Jones, "Using Simplex codes to improve OTDR Sensitivity," *IEEE Photonics Technol. Lett.* **5**(7), 822–824 (1993).
22. M. Nazarathy, S. A. Newton, R. P. Giffard, D. S. Moberly, F. Sischka, W. R. Trutna, and S. Foster, "Real-time long range complementary correlation optical time domain reflectometer," *J. Lightwave Technol.* **7**(1), 24–38 (1989).
23. G. Bolognini, J. Park, M. A. Soto, N. Park, and F. Di Pasquale, "Analysis of distributed temperature sensing based on Raman scattering using OTDR coding and discrete Raman amplification," *Meas. Sci. Technol.* **18**(10), 3211–3218 (2007).
24. M. A. Soto, P. K. Sahu, S. Faralli, G. Bolognini, F. Di Pasquale, B. Nebendahl, and C. Rueck, "Distributed temperature sensor system based on Raman scattering using correlation-codes," *Electron. Lett.* **43**(16), 862–864 (2007).
25. M. A. Soto, P. K. Sahu, G. Bolognini, and F. Di Pasquale, "Brillouin-based distributed temperature sensor employing pulse coding," *IEEE Sens. J.* **8**(3), 225–226 (2008).
26. M. A. Soto, G. Bolognini, and F. Di Pasquale, "Analysis of optical pulse coding in spontaneous Brillouin-based distributed temperature sensors," *Opt. Express* **16**(23), 19097–19111 (2008).
27. G. Bolognini and M. A. Soto, "Optical pulse coding in hybrid distributed sensing based on Raman and Brillouin scattering employing Fabry-Perot lasers," *Opt. Express* **18**(8), 8459–8465 (2010).
28. D. Grodensky, D. Kravitz, N. Arbel, N. Levanon, and A. Zadok, "Incoherent pulse compression in laser range finder," *Proc. SPIE* **9080**, 90800M (2014).
29. A. Minardo, R. Bernini, and L. Zeni, "A simple technique for reducing pump depletion in long-range distributed Brillouin fiber sensors," *IEEE Sens. J.* **9**(6), 633–634 (2009).

1. Introduction

Brillouin optical time-domain analysis (BOTDA) [1] has been extensively used for distributed optical fiber sensing of physical quantities such as temperature and strain. In the conventional BOTDA technique, an optical pulse is used as pump wave providing Brillouin gain/loss to a counter-propagating (CW) light that is used as probe wave. When the pump-probe frequency offset falls within the Brillouin gain/loss spectrum, the probe wave is amplified/depleted by the pump pulse during the interaction process. As the spectral position of the Brillouin gain/loss spectrum (BGS/BLS) depends linearly on the fiber temperature and strain, any change in these quantities can be detected by measuring the spectral shift of the peak gain frequency [1]. The possibility to reach very long sensing ranges is one of the most attractive features of BOTDA sensing owing to its unique ability to perform high-quality measurements over several tens of kilometers [2], while keeping a spatial resolution in the meter scale. One of the main limitations on the sensor performance is imposed by the fiber losses, which highly reduce the pump and probe powers at very long sensing ranges, thus leading to an exponential decay of the signal-to-noise ratio (SNR) on the sensor response [2]. In order to overcome such a limitation, while maintaining a given spatial resolution, higher peak power pump pulse can be used; however, the peak level cannot be increased indefinitely due to the onset of detrimental nonlinear effects, such as modulation instability [3] or forward stimulated Raman scattering [4]. These nonlinear effects prematurely deplete the pump, reducing the effective

Brillouin gain along the sensing fiber, and restricting the maximum sensing length. To avoid affecting the sensor performance, the maximum pump pulse power tolerated in the sensing fiber is limited to about 100 mW (for fibers longer than the asymptotic nonlinear effective length $\alpha^{-1} \approx 22$ km) [3,4]. On the probe wave side, the power of the CW probe is ultimately limited by the onset of amplified spontaneous Brillouin scattering, which also eventually sets a limit to the SNR on the measurements [5]. To overcome all those limitations to the performance of long-range Brillouin sensors, alternative solutions such as distributed Raman amplification [6–8] and optical pulse coding [9–15] have been proposed, providing a huge improvement in the sensor performance, especially when both techniques are combined in the same system [16,17]. The situation becomes even more critical and demanding in terms of SNR when the real remoteness of the sensor is extended using a linear fiber-loop configuration [17,18], in which half of the fiber is used for sensing while the second half, paired to the sensing segment, is used to convey the probe to the most remote sensing location, i.e. to the end of the sensing fiber. Since the total fiber length in this case is doubled, the probe power experiences a very large attenuation during propagation before reaching the receiver (e.g. 40 dB losses in a 200 km-long fiber-loop for 100 km sensing). Combining pulse coding and Raman amplification, a real remoteness of 120 km sensing range has been demonstrated in 240 km-long optical fiber loop using 5 m spatial resolution and 1.9 MHz frequency standard deviation using 2040 averages [17], thus leading to the best performance so far reported in a Brillouin sensor, proved by a record figure-of-merit (FoM) of 300,000 [2].

A substantial amount of research has been carried out on coding-based schemes aiming at enhancing the performance of Brillouin distributed sensors, while avoiding, if possible, the use of distributed optical amplification. Besides enhancing BOTDA systems for long range [9–15], optical pulse coding has also been applied to high spatial resolution Brillouin sensors, based for instance in correlation-domain [19]. While coding schemes based on incoherent pulse compression [19,20] have efficiently been used in high spatial resolution sensors, demonstrations in long-range BOTDA have been classically based on unipolar sequences, such as Simplex [9] or Golay [11] codes. Two kinds of pulse coding schemes have been recently proposed as a new breach in long range sensing: *bipolar codes* [12] and *time/frequency or colored codes* [13–15]. Both coding schemes offer improved SNR enhancement in comparison to traditionally-used unipolar coding schemes [9–11]. In particular, while colored codes can provide an additional 1.5 dB enhancement when compared to optimal unipolar codes, this improvement is increased up to 3 dB (1.5 dB over time/frequency codes) for bipolar Golay codes [12], leading to an overall SNR improvement of about 13.5 dB when using bipolar Golay sequences of 512 bit.

In this paper serious and very specific detrimental effects resulting from pump depletion in bipolar coded BOTDA sensors are identified. These effects find the same origin as the well-known non-local effects affecting conventional BOTDA schemes [5], but turn out to have an entirely different and specific impact. They are due to the pump power misbalance between the +1's and -1's code elements resulting from pump depletion/excess amplification, which breaks the linearity required in bipolar coding. In order to increase the robustness of bipolar codes against such pump depletion issues, a novel three-tone probe scheme is proposed, allowing for at least 12.5 dB probe power improvement when compared to existing implementations. Experimental results here demonstrate the feasibility of the proposed method to reach a sensing range of 100 km (real remoteness) in a 200 km-long fiber-loop, with 2 m spatial resolution and 0.9 MHz frequency uncertainty on the Brillouin frequency shift when using 1000 averages per trace. The improvement brought by the proposed method and its implementation is quantified by a figure-of-merit of 380'000, which, to the best of our knowledge, constitutes the highest FoM so far reported in a Brillouin distributed fiber sensor.

2. Bipolar Golay coding in BOTDA using three-tone probe scheme

2.1 Principle of bipolar Golay coding and impact of pump depletion on BOTDA sensing

The benefits of optical pulse coding in distributed fiber sensing have been demonstrated and widely improved for many years. Traditionally the method is based on the intensity modulation of a pump wave, enabling a natural incorporation of unipolar code sequences (containing 0's and 1's) into conventional distributed fiber sensors. This is the case of conventional optical time-domain reflectometers (OTDR) [21,22], Raman-based distributed sensors [23,24], Brillouin-OTDR sensors [25,26], hybrid schemes [27], and laser range finder [28], in which pulse coding has shown important improvement with respect to conventional schemes. In addition, unipolar coding has also been used in BOTDA sensing [9–11]; however, the Brillouin gain and loss processes can offer the unique possibility to implement another kind of coding scheme: the so-called *bipolar coding* [12] (i.e. sequences containing +1's and -1's). In this scheme pump pulses at frequencies higher than the probe represent the '+1' code elements (inducing Brillouin gain on the probe), while pump pulses at lower frequencies represent the '-1' code elements (inducing Brillouin loss). In [12] a bipolar complementary-correlation Golay coding method has been proposed for BOTDA sensing, offering a coding gain equal to \sqrt{L} (L being the code length), which represents 3 dB more SNR enhancement than the one obtained by optimal unipolar codes.

The use of bipolar Golay codes in Brillouin sensing consists of three steps [12,22]: 1) two L -element Golay complementary pair sequences A_k and B_k are consecutively generated and launched into the sensing fiber ('+1' elements are generated by spectrally up-shifted pump components and '-1' elements are generated by down-shifted pump components). Pulse sequences are convolved with the measured fiber impulse response h_k (where h_k corresponds to the measured Brillouin gain distribution at the scanned pump-probe frequency offset and obtained by an infinitely narrow single pulse), leading to two different responses: $A_k \otimes h_k$ and $B_k \otimes h_k$. 2) Each of those two responses are correlated with the corresponding original (ideal) sequence launched into the fiber (i.e. A_k and B_k , respectively). 3) Finally the result of these correlations are summed up to get the final (decoded) fiber impulse response h_k , but with enhanced SNR. The whole process can be represented mathematically as [22]:

$$\begin{aligned} A_k * (A_k \otimes h_k) + B_k * (B_k \otimes h_k) &= (A_k * A_k) \otimes h_k + (B_k * B_k) \otimes h_k \\ &= \{(A_k * A_k) + (B_k * B_k)\} \otimes h_k \end{aligned} \quad (1)$$

where the * sign denotes correlation.

From Eq. (1) it can be seen that the coding/decoding process is mathematically equivalent to interrogate the fiber impulse response h_k with the sum of the autocorrelations of the two sequences. One of the main properties of Golay codes is their complementary correlation functions [22], which means that the autocorrelations of sequences A_k and B_k have the same main correlation peak, but sidelobes showing opposite signs, as depicted in Fig. 1. This figure shows an example of the autocorrelation functions of A_k and B_k in case of 8-bit return-to-zero bipolar Golay codes. As shown in Fig. 1(c), the sum of the autocorrelation functions reinforces the main correlation peak and cancels out the sidelobes.

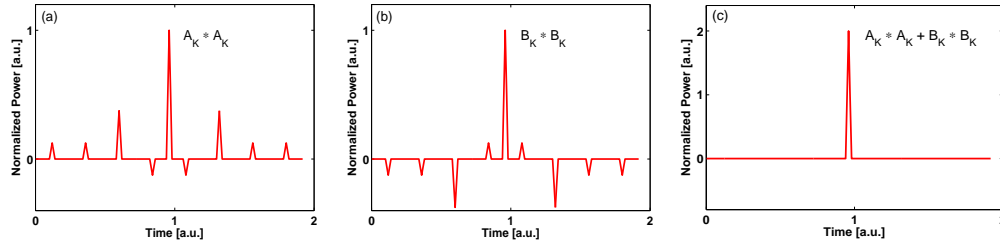


Fig. 1. Autocorrelation of the (a) first and (b) second 8-bit bipolar Golay code sequences using return-to-zero format. (c) Interrogation function of bipolar complementary-correlation Golay codes, resulting from the sum of the two autocorrelations.

The autocorrelation function represented by Eq. (1) and shown in Fig. 1(c) can be interpreted as the temporal shape of the pump (i.e. equivalent to a single pulse) in the conventional BOTDA scheme, interrogating the local Brillouin gain along the fiber. However, in real situations when the code sequences propagate along very long sensing fibers, coded pump pulses at higher frequency ('+1' code elements) can experience a significant power depletion as a result of the long Brillouin interaction length, while pulses at lower frequency ('-1' code elements) can reversely experience an excessive Brillouin amplification. Consequently, a serious power misbalance is induced between -1's and +1's, breaking the linear relation between code elements. This results in correlation sidelobes that can no longer be cancelled out perfectly, leading to a final autocorrelation function showing uncompensated and detrimental sidelobes. Figure 2 exemplifies the situation in the case of a 20% depletion when using 8-bit bipolar Golay sequences. The residual correlation sidelobes are clearly seen in Fig. 2(c). Note that, for the sake of clarity, the figure here only describes the impact of pump power misbalance on the decoding process, while the additional measurements errors resulting from a 20% pump depletion [5] are not addressed but remain present.

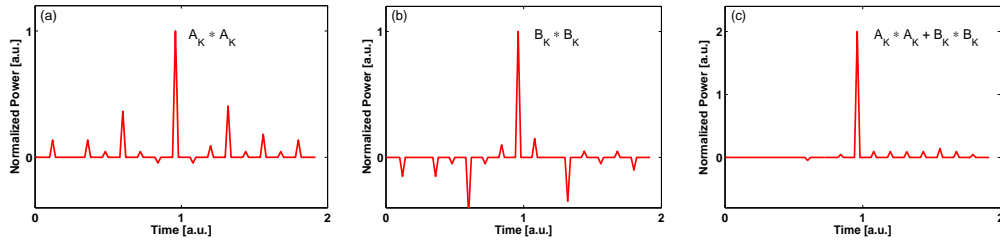


Fig. 2. Impact of 20% pump depletion on the autocorrelation functions of bipolar Golay codes. Autocorrelation of the (a) first and (b) second 8-bit bipolar Golay code sequences using return-to-zero format. (c) Interrogation function resulting from the sum of the autocorrelations.

It is worth mentioning that the residual correlation sidelobes carry the Brillouin gain/loss information from their corresponding positions (i.e. from the entire fiber section covered by the autocorrelation function), contaminating the local spatial information that should only be attributed to the main correlation peak. The fiber length covered by the residual sidelobes depends on the length of bipolar Golay sequences; the sidelobes can therefore spread over several kilometers when the code length is very long (e.g. in the case of return-to-zero 512 bits with 20 ns pulses and 20% duty cycle [10], the sidelobes can cover a length of about 10.2 km). Figure 3(a) shows the residual sidelobes obtained for 10% (blue) and 20% (green) pump depletion. If the integrated power confined in all the residual sidelobes is small enough, most of the measured Brillouin interaction (i.e. the information in the BOTDA trace) can be attributed to the sensor response resulting from the main correlation peak, leading to correctly decoded traces. However, when the total (integrated) power confined in the residual sidelobes approaches the power in the main correlation peak (e.g. < 10 dB difference), the measured local Brillouin gain spectrum associated to a given fiber location will be highly affected by

the BGS of neighboring fiber sections, screening the real local information contained in the measurements.

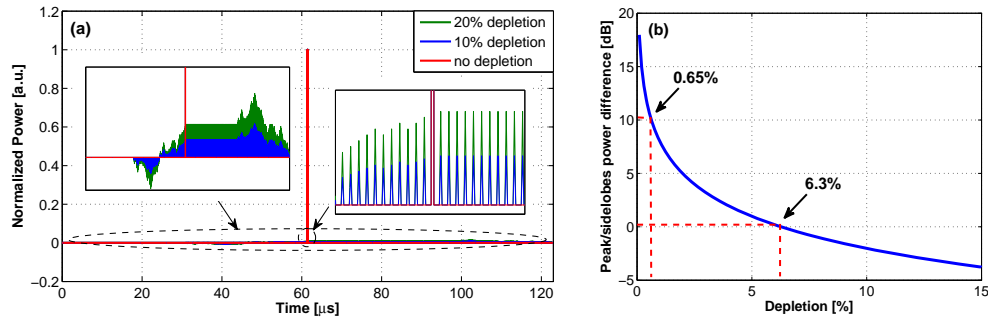


Fig. 3. (a) Autocorrelation function of bipolar Golay codes in case of no depletion (red curve), 10% depletion (blue curve) and 20% depletion (green curve). Inset: zoom of correlation sidelobes over the doubled code length. (b) Power difference (in dB scale) between the main correlation peak and sidelobes as a function of the depletion level.

Figure 3(b) shows the power difference (in dB scale) between the main correlation peak and the integrated power over all the residual sidelobes as a function of the depletion level. It can be seen that with a pump depletion/amplification higher than 6.3% (i.e. 12.6% of power misbalance between ‘ -1 ’ and ‘ $+1$ ’ code elements), the contribution from the correlation sidelobes will completely dominate, resulting in a system offering an effective spatial resolution equivalent to twice the total code length (being typically in the kilometer scale). Considering a safe power margin of 10 dB between the contributions of the main autocorrelation peak and the residual sidelobes, the system can only tolerate a pump depletion lower than 0.65% (i.e. 1.3% of power misbalance). This means that a very low probe power is required to alleviate the information distortion from the decoding process due to pump depletion/amplification, and to therefore grant a correct decoding of bipolar Golay-coded BOTDA traces. Unfortunately, this low probe power restriction causes a severe penalty to the SNR of the system, annihilating all benefits from bipolar pulse coding.

It is worth mentioning that the implementation of bipolar coding using a single-probe tone is likely to be affected by strong misbalance between the -1 ’s and $+1$ ’s, inducing large residual sidelobes. This is actually the case of the scheme reported in [12], in which the impact of the high-amplitude sidelobes on the retrieved Brillouin frequency shift (BFS) was not observed due to the use of very long fiber spools (~ 50 km length) having no large longitudinal variations of the BFS over the fiber effective length (i.e. last ~ 22 km length). Note that in such a case, the BGS information provided by the residual sidelobes overlaps the BGS attributed to the main correlation peak, making any contamination indiscernible. As experimentally demonstrated in Section 4, the use of a single-tone probe induces a strong deviation of the retrieved BFS, which is only observable if the BFS varies in the last kilometers of fiber. This distortion can be highly reduced by a novel scheme, based on a three-tone probe, which is described here below in Section 2.2.

2.2 Proposed scheme based on a three-tone probe

In order to mitigate the impact of the correlation sidelobes resulting from depletion while maintaining high probe powers, a novel implementation based on a three-tone probe scheme is proposed in this paper. In this approach the probe wave consists of three frequency components of equal intensity, as illustrated in Fig. 4. The frequency difference between adjacent tones has to be set to twice the frequency used to generate the pump components and to subsequently perform the scan over the Brillouin gain/loss spectrum. While the central spectral component corresponds to the coded probe signal that is detected in the receiver, the role of the upper and lower sidebands is just to compensate for the depletion/amplification affecting the pump pulses [5,29]. This way, the additional probe waves are actually expected

to reduce significantly the power misbalance between the two pump spectral components even when using very long sensing fibers. This leads to a decoding process generating a strong main correlation peak and low-amplitude sidelobes. As a consequence, the probe power launched into the fiber can be significantly raised, offering the possibility to monitor extended fiber sensing ranges and fully preserving the advantages associated to bipolar codes.

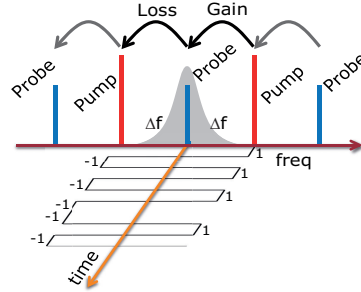


Fig. 4. Principle of proposed bipolar coded BOTDA system with a three-tone probe.

3. Experimental setup

The experimental setup that has been implemented to validate the proposed method is shown in Fig. 5. The light from a distributed feedback laser (DFB) is split into pump and probe branches using an optical splitter. In the pump branch (upper arm in the figure), the continuous-wave light is injected into a high extinction ratio (40 dB) electro-optic modulator (EOM1), operating at null transmission point to generate a carrier-suppressed double-sideband (SC-DSB) wave, using a varying RF modulating frequency performing a scan over the BGS of the sensing fiber. A programmable wavelength-selective filter (WSF) with a 3 dB bandwidth of 10 GHz is used to separate the two modulation sidebands, which are then intensity-modulated with 512-bit return-to-zero sequences using EOM2 and EOM3, driven by arbitrary waveform generators (AWG). The pulse width is set to 20 ns, which corresponds to a spatial resolution of 2 m, and to a duty cycle of 16.7% in return-to-zero format [10]. The two pump pulse sequences are properly synchronized and re-combined with equalized powers using a coupler, building this way the full bipolar Golay coded sequence. Compared to the scheme reported in [12], which uses a dual-parallel Mach Zehnder modulator, this new implementation makes the system much more stable and reliable. Since the aim of this paper is to measure very long sensing ranges, another modulator (EOM4) is then used to gate the coded sequences, and thus double (in dB scale) the pump pulses extinction ratio to reach some 80 dB. After a polarization alignment, the bipolar Golay codes are amplified up to 18 dBm peak power and launched into a 100 km-long sensing fiber made of four drums of fiber having similar Brillouin frequency shifts.

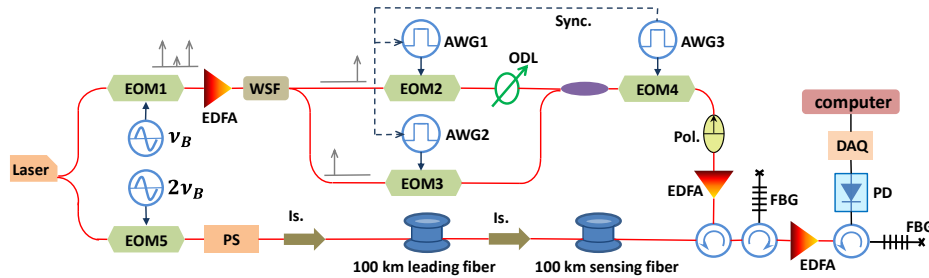


Fig. 5. Experimental setup of the proposed method based on a three-tone probe scheme; EOM: electro-optic modulator. AWG: arbitrary waveform generator; ODL: optical delay line; Pol.: polarizer; PS: polarization switch; Is.: isolator; EDFA: erbium-doped fiber amplifier, FBG: fiber Bragg grating; DAQ: data acquisition card; PD: photodetector.

In the other branch (lower arm in Fig. 5), a probe wave with three equalized spectral tones is generated by intensity modulation using EOM5 biased at the quadrature transmission point. The modulation frequency in this case has to be synchronized with the one applied to EOM1, being simply multiplied by a factor 2. A polarization switch (PS) is then used to minimize the impact of the polarization-dependent Brillouin gain. The three-tone probe is carried over a 100 km-long leading fiber. An optical isolator has been placed in-between sensing and leading fibers to restrict the pump-probe Brillouin interaction only into the sensing fiber, avoiding any kind of unwanted interaction in the leading fiber.

In the receiver block, two tunable narrowband fiber Bragg gratings (FBG), centered at the optical carrier frequency, are used to filter out the two additional probe sidebands and the strong integrated Rayleigh backscattering originating from the long pump sequences. An EDFA is used between the two FBGs as a linear-gain pre-amplifier. The first FBG actually prevents the EDFA from saturating by the strong Rayleigh backscattered light (which in this case is 512 times larger than in the single-pulse case), while the second FBG filters out residual unwanted components and large part of the amplified emission noise introduced by the EDFA. The signal is then detected by a 125 MHz photoreceiver (PD) connected to a fast data acquisition (DAQ) system.

4. Experimental results and discussion

In order to evaluate the probe power enhancement provided by the proposed method, the pump depletion levels obtained by the technique have been experimentally compared with the use of the traditional single-tone probe scheme [12], which is simply realized by turning off the EOM5 modulation. Figure 6 shows the measured depletion as a function of the probe power, for the two cases. Experimental results verify that the use of the proposed three-tone probe scheme leads to reduced levels of pump depletion even with probe powers close to the mW level. It should be mentioned that during the measurement process a complete suppression of pump depletion was reached when the three probe tones were fully equalized. Nevertheless, thermally-induced drifts in the operation point of the electro-optic modulator (EOM5 in Fig. 5) can easily break the power equalization between the three tones, thus inducing some residual level of depletion. Therefore in order to provide a more realistic value of depletion, a 0.5 dB power difference between the optical carrier and the two sidebands has been deliberately introduced during the measurement (note that this power equalization can be realistically reached using a proper PID controller to stabilize the EOM). Figure 6 shows that for a given level of depletion, the proposed three-tone probe technique offers an average 12.5 dB improvement to the input probe power permitted by the system (note that a larger enhancement was actually obtained when a lower power difference between probe tones was reached during the experiment). This is actually a remarkable improvement, which has a direct impact on the SNR of the measurements [2], thus making better use of the advantages provided by bipolar pulse coding. It is important to mention that this kind of improvement is expected not only in complementary Golay codes, as demonstrated here, but in any other kind of bipolar code that can potentially be adapted to BOTDA sensing. Based on the results reported in Fig. 6, and in order to keep the required pump depletion below 0.65% (thus constraining the impact on the decoding process, as reported in Section 2.1), a long-range BOTDA sensor based on a three-tone probe scheme can safely use up to -11 dBm/tone to obtain measurements without distortions resulting from pump depletion.

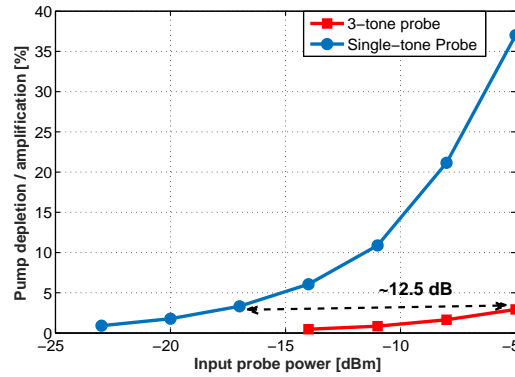


Fig. 6. Experimental levels of depletion/amplification measured as a function of the input probe power for the conventional single-probe scheme and the proposed three-tone probe scheme. A margin of 0.5 dB power misbalance between the 3 spectral components has been imposed during the measurement.

In case of a 200 km-long fiber-loop, as implemented here, the onset of amplified spontaneous Brillouin scattering limits the power launched into the leading fiber to 7 dBm/tone. In order to increase this power limit, fibers with different Brillouin frequencies have been used as leading fiber, conveying the probe up to a remoteness of 100 km. With no impact on the demonstration addressed in this paper this has enabled the use of an optimum probe power of 10 dBm/tone, which results in -11 dBm/tone entering into the sensing fiber (note that during measurements the power equalization between the three-probe tones has been maintained to a much lower level than the 0.5 dB margin described in Fig. 6, and therefore the used probe power can safely ensure depletion levels much below the 0.65% limit). Under such a condition, the last 10 residual coded pump pulses of a 512 bit sequence have been measured after propagating along the 100 km sensing fiber and are shown in Fig. 7(a) for the two cases: single-tone probe (solid blue line) and three-tone probe (solid red line). As it can be seen, there is no evident pump depletion in the three-tone probe scheme; however, the residual pump is clearly depleted/amplified by 10.7% in the conventional single-tone system. In order to know the temporal shape of the interrogation function, the measured pulse sequences have been cross-correlated with their respective ideal pulse shapes and results have been summed up. This is actually the exact procedure followed by the decoding process, as described in Eq. (1). As a result of this decoding, the real interrogation function resulting from depletion shown in Fig. 7(a) has been obtained and graphed in Fig. 7(b). The distortion in the correlation function is evident from the figure (blue curve), and agrees very well with the theoretical behavior described in Fig. 2 and Fig. 3(a). However, with the use of the proposed three-tone probe scheme (red curve), the sidelobes have been substantially reduced. Actually, the power contribution of the sidelobes has been estimated by integrating the experimental interrogation functions in Fig. 7(b). Results indicate that, in the conventional single-probe scheme, the total power contained in the sidelobes is 1.9 dB higher than the power measured in the main correlation peak (in well agreement with the -2.3 dB obtained from Fig. 3(b)); this means that most of the contribution in the measured BOTDA traces can be attributed to the residual uncompensated sidelobes and not to the main correlation peak. On the other hand, with the use of the proposed scheme, the integrated power within the sidelobes has been reduced down to 21.5 dB below the power contained in the main peak. This, according to Fig. 3(b), corresponds to a pump depletion below 0.1%, which actually has led to an unobservable depletion level (red curve in Fig. 7(a)).

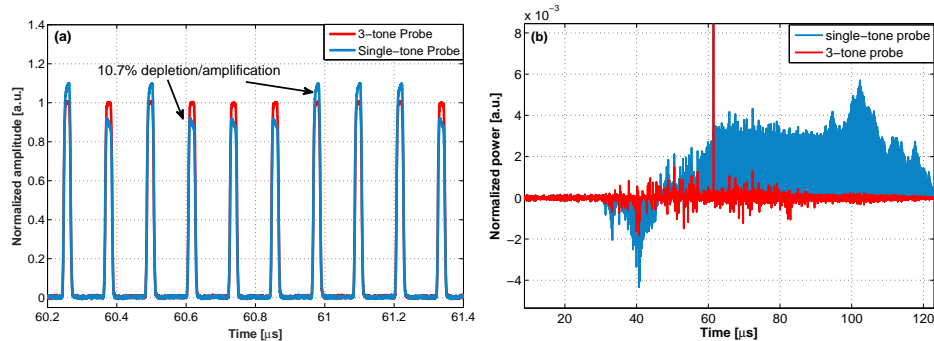


Fig. 7. Comparison of the impact of pump depletion on bipolar Golay-coded BOTDA sensors with single-tone probe and three-tone probe (a) Normalized amplitude of bipolar Golay-coded pulses after propagation along 100 km-long fiber. (b) Sum of autocorrelation functions resulting from the decoding process in bipolar Golay coding.

Figure 8 shows the BFS profile obtained along the 100 km sensing fiber with 1000 averages per trace. Note that the BFS over the entire sensing section is not strictly uniform, showing longitudinal variations within a 20 MHz range. However, these variations are actually narrower than the full-width at half-maximum of the Brillouin gain, and therefore the measurement scenario still ensures a continuous depletion of the pump power all over the sensing fiber, thus providing a good condition to evaluate the effectiveness of the proposed method. Calculating the standard deviation of the BFS, the frequency uncertainty has been found to be 0.9 MHz at 100 km distance. Note that the thickness of the BFS trace in the figure only results from the periodic coiling strain in the fibers, inducing oscillations of the BFS along the entire sensing range. This way, taking full benefit of the high coding gain of bipolar Golay codes (13.5 dB for 512 bits) and of the enhanced probe power provided by the three-tone probe, the system can compensate for ~42 dB fiber loss along the 200 km-long loop (21 dB in the sensing fiber), without the need of other advanced techniques such as distributed optical amplification. This has led to a record sensing performance, evaluated by a figure-of-merit [2] of 380'000.

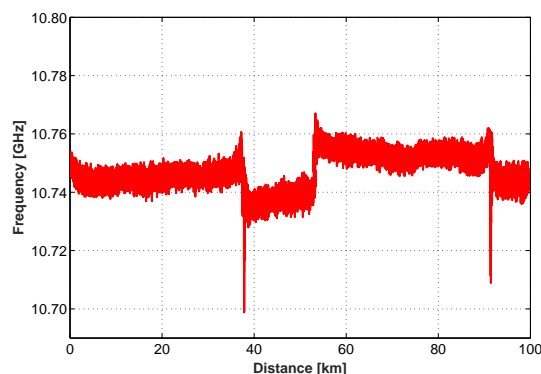


Fig. 8. BFS profile along 100 km fiber obtained by a bipolar Golay-coded BOTDA sensor using a three-tone probe.

The use of fibers with different and relatively uniform BFS in the last 20 km of fiber (corresponding to the effective length section where pump depletion is the strongest) actually provides a clear scenario to evaluate distortions in the BFS, potentially resulting from pump depletion. Figure 9(a) compares the BFS obtained at the end of the sensing fiber using a single-tone probe and the proposed three-tone probe. The figure shows that the single-tone case (blue curve) induces a large frequency error in the BFS estimation around the transition zone between the two last fiber drums. This BFS error can actually be explained by the high

pump depletion (10.7%) and large autocorrelation sidelobes (covering a fiber section of ~ 12 km) resulting from the single-tone probe. As previously described, the depletion of 10.7% obtained in this case by the single probe scheme results in only -1.9 dB difference between the contribution of correlation peak and sidelobes (integrated power over them), making those sidelobes dominate over the main peak. This condition leads to BOTDA traces that contain the cumulated Brillouin gain/loss information over an entire fiber section twice as long as the code sequence length. This way the integrated BGS information carried by the residual sidelobes highly contaminates the local BGS information interrogated by the main correlation peak, inducing the distortions shown by the blue curve in Fig. 9(a). For instance, when the correlation peak passes through the point at 92 km (inside the last fiber spool), the actual BGS also contains the information of the fiber drum before the transition zone, which has higher BFS, forcing the BFS retrieved by fitting to be up-shifted. On the other hand, the red curve in the figure has been obtained with the proposed three-tone probe scheme.

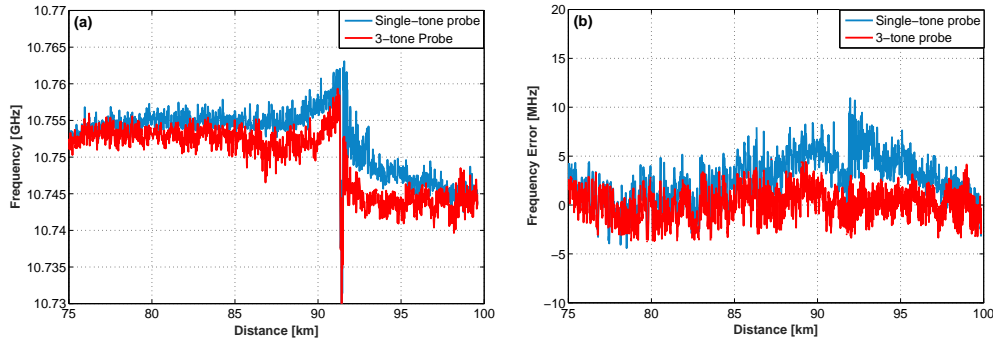


Fig. 9. (a) BFS profiles along the last 25 km range, comparing the use of a single-tone probe and a three-tone probe. (b) Frequency error in the BFS profile measured in the two schemes. Here a reference BFS profile has been measured by swapping the fiber ends, thus ensuring that the local Brillouin interaction is not affected by nonlocal effects.

To demonstrate that the BFS profile obtained with the proposed method is correct, the measurement was repeated by swapping the two ends of the sensing fiber, thus securing that a reference BFS profile could be measured (within the section of interest) using a very low local probe power (i.e. inducing negligible pump depletion). For the sake of visual clarity, this reference BFS profile is not represented in Fig. 9(a); however, it has been used to calculate the absolute frequency error in the BFS estimation in the two cases. Figure 9(b) demonstrates that while an error of about 6-9 MHz affects the BFS estimation in the single-probe scheme, as a consequence of pump depletion, the proposed method based on three-tone probe considerably reduces this frequency error (actually the root-mean-square in this case has been calculated to be 1.3 MHz, being essentially determined by the frequency uncertainty of the system).

In order to verify that the proposed method is not affected by nonlocal effects distorting the local spatial information measured by the system (as it would happen with strong depletion levels), a 2 m hot-spot placed at the end of the 100 km sensing range has been measured. For this purpose, 2 m of fiber have been heated up to 45°C , while the rest of the sensing fiber has been maintained at ambient temperature (26°C). Figure 10 shows a correct hotspot detection, revealed by a Brillouin frequency variation of 19 MHz along 2 m of fiber. This result demonstrates the capability of the system to provide a metric spatial resolution at 100 km distance with no distortion and no detrimental effects resulting from pump depletion.

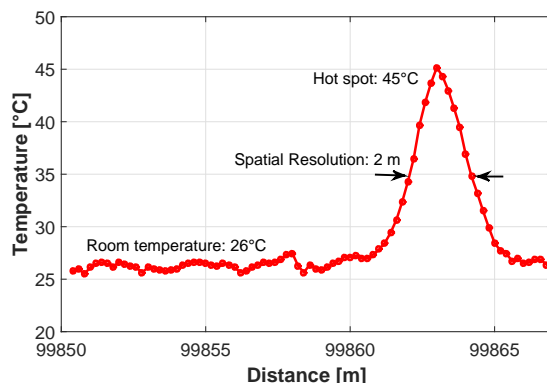


Fig. 10. Demonstration of a 2 m-long hotspot detection at 100 km distance (real remoteness from the sensor) in a 200 km-long fiber loop configuration.

5. Conclusion

In this paper the effects of pump depletion/excess amplification in Brillouin distributed fiber sensors using bipolar coding have been analyzed and investigated. Theoretical and experimental results have shown that bipolar coding actually imposes very demanding conditions to the maximum probe power that can be launched into the sensing fiber to keep pump depletion below very low levels ($< 0.65\%$). In order to overcome the probe power limitation and to take full advantage of bipolar pulse coding, a novel scheme based on a three-tone probe is proposed. The capability of the proposed method to provide almost perfect Brillouin gain/loss compensation ($< 0.1\%$ difference) and mitigate pump depletion issues has been experimentally demonstrated. The method offers several advantages: *i*) possibility to use any kind of bipolar code sequence offering high SNR enhancement, *ii*) mitigation of pump depletion issues specific to bipolar codes that are more restrictive than the common depletion distortion, *iii*) keep the linearity required by pulse coding methods, and *iv*) support of high probe powers (more than 12.5 dB enhancement with respect to the state-of-the-art based on a single-tone probe), which is only limited by the onset of amplified spontaneous Brillouin scattering. The combination of all these advantages, in addition to the large SNR enhancement provided by bipolar Golay codes, has enabled to compensate 42 dB of fiber loss in a 200 km-long loop scheme (representing a 21 dB dynamic range in the BOTDA traces), with no need of distributed optical amplification. To the best of our knowledge the experimental validation of the proposed method represents to date a record figure-of-merit of 380'000.

Acknowledgments

The authors acknowledge the support from the Swiss Commission for Technology and Innovation (Project 13122.1). Z. Yang acknowledges the China Scholarship Council and BUPT Excellent Ph.D. Students Foundation (CX201431) for supporting his stay at EPFL.